Structure of Skin Layer in Injection-Molded Polypropylene

MITSUYOSHI FUJIYAMA and TETSUO WAKINO, *Polymer Research Laboratory, Research Division,* and YOUTOKU KAWASAKI, *Quality Control Section, Resins Division, Tokuyama Soda Co., Ltd., Tokuyama-shi, Yamaguchi-ken 745, Japan*

Synopsis

The structure of skin layer in injection-molded polypropylene which displayed a clear two-phase structure of skin and core has been studied by means of wide-angle x-ray diffraction, small-angle x-ray scattering, melting behavior, density, dynamic viscoelasticity, and tensile test. In skin layer, the c-axis and a*-axis were highly oriented to the machine direction (MD), and the plane of the lamellar structure of about 160 Å in thickness was in normal to MD. The density was about 0.907 g/cm^3, which was nearly the same as that of core layer. Although the majority of crystallites melted in the same temperature range as in that of the core layer, there was about 5.3% higher temperature melting structure (T_m = 182°C). The dynamic tensile modulus E' in MD decreased more slowly with increasing temperature than that of the core layer and held high modulus in the range of ca. 30°C, just above the temperature at which E' of the core layer suddenly dropped. E' in MD was higher than that in TD in the temperature range below 33°C, which was slightly higher than the primary absorption temperature, and the order reversed above 33°C. The tensile yield stress in MD was 1.5 times higher than that of the core layer. The skin layer in MD ruptured just after yielding and did not show necking. The tensile yield stress in TD was about half of that in MD and about 0.7 times that of the core layer. The necking stress in TD was about 0.6 times that of the core layer. In general, a polypropylene melt crystallizes under a high shear stress in injection molding. From these facts, it was concluded that the skin layer is composed of so-called "shishkebab"-like main skeleton structures, whose axis is parallel to MD, piled epitaxially with a*-axis-oriented imperfect lamellar substructure.

INTRODUCTION

An injection-molded polypropylene shows a clear two-phase structure of skin and core when its cross section is observed with a polarizing microscope. The thickness of the skin layer varies widely with the kind of resin and molding conditions, and physical properties such as elastic modulus, yield strength, and mold shrinkage systematically change accordingly.[1-5] It is important therefore to clarify the structure of the skin layer which governs the physical properties of injection moldings.

Clark[6] showed from electron microscopy and small-angle x-ray scattering measurement that lamellae are perpendicular to MD at the surface of injection-molded acetal polymer. He[7] also found from x-ray diffraction measurement that the skin layer in injection-molded polypropylene has a mixed c-axis and a*-axis orientation which he called "bimodal" and explained its formation by assuming that the c-axis-oriented component was formed first and the a*-axis component was formed by epitaxial overgrowth on the c-axis-oriented substrate.

Journal of Applied Polymer Science, Vol. 35, 29–49 (1988)

CCC 0021-8995/88/010029-21$04.00

Kantz et al.[1] made x-ray diffraction measurements on the skin layer in injection-molded polypropylene from various directions and found that crystallites are biaxially oriented to MD and the tensile yield strength and mold shrinkage in MD were higher as the skin layer was thicker.

Mencik and Fitchmun[8] found from polarizing microscopy and x-ray diffraction measurement that injection-molded polypropylene is composed of five layers, whose thickness changed according to molding conditions. The third layer, which was an oriented layer, showed a mixed c-axis and a*-axis orientation to MD. They explained its formation by assuming that lath-like crystallites whose a*-axes oriented to MD were formed first and the c-axis-oriented component was formed by unfolding the molecular chains of the a*-axis-oriented component by shearing force. They obtained a two-spot diffraction pattern in MD in a small-angle x-ray scattering measurement of the third layer.

Matsumoto et al.[9] found using polarizing microscopy that injection-molded polypropylene is composed of at least six layers, and the thickness of oriented layer was governed mainly by resin temperature and mold temperature.

These studies intend to analyze the structure of the skin layer in injection-molded polypropylene on the basis of structural analysis. This study aimed to clarify the structure (mainly of the skin layer) of an injection-molded polypropylene from the measurements of thermal property, mechanical property, and density as well as polarizing microscopy and x-ray diffraction.

EXPERIMENTAL

Injection Molding

The resin used was Tokuyama Polypro YE-120 (homoisotactic polypropylene, MFI = 1.6 dg/min, manufactured by Tokuyama Soda Co., Ltd.). Flexural test specimens (ASTM D790) were injection molded using an 8 oz NIKKO ANKERWERK V22A-120 type reciprocating-screw injection-molding machine. The shape of the test specimen is shown in Figure 1. A polymer reservoir was provided to make resin flow in the specimen uniform. Although molding conditions were changed widely, specimens molded under the following conditions which showed the most clear skin/core structure were used for structural analyses:

cylinder temperature;	160°C, 190°C, 200°C, 190°C
injection pressure;	300 kg/cm^2
injection speed;	33 cc/s
mold temperature;	40°C
cooling time;	10 s

For comparison, unoriented specimens were prepared by compression molding under conditions of melting temperature of 215°C, compression pressure of 100 kg/cm^2, compression time of 10 min, and cooling by water.

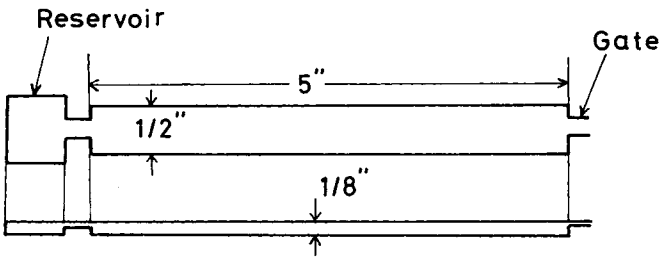

Fig. 1. Shape of test specimen.

Measurements

Observation of Crystalline Texture with Polarizing Microscopy

A slice of about 0.1 mm thickness was cut perpendicular to MD from the central part of the specimen and was observed with a universal projector (Olympus UT350) under crossed polars with magnifications of 10 × and 50 × .

Wide-Angle X-ray Diffraction

Since the thickness of the skin layer was about 0.6 mm when observed with polarizing microscope (see Fig. 2), skin layer and core layer specimens of about 0.4 mm thickness were sliced from, respectively, the surface and the center of the central part of the flexural specimen parallel to its surface. The diffraction of through view (THRU) was taken on one specimen piece and those of edge view (EDGE) and end view (END) were taken on a pile of five pieces. X-ray diffraction photographs were taken using a Rigaku Denki RU-200 diffractometer with Ni-filtered Cu-Kα radiation at 45 kV × 200 mA for 10 min and a sample-to-film distance of 45 mm. Using a goniometer, 2θ scan was carried out at a scan speed of 4°/min and azimuthal scans of (110) and (040) reflections were carried out at a scan speed of 8°/min, and crystalline orientation functions f_a^*, f_b, and f_c were calculated according to Wilchinsky's method.[10] Furthermore, 2θ scan was carried out for THRU using a rotating specimen table and the crystallinities of the skin and core layers were calculated according to Hearman's method.[11]

Small-Angle X-ray Scattering

The small-angle x-ray scattering of THRU was taken on the same specimen as used for wide-angle x-ray diffraction by means of photographic and goniometric methods. The photographic method was carried out using pin-hole slits with Ni-filtered Cu-Kα radiation at 40 kV × 20 mA for 7 h and a sample-to-film distance of 250 mm. The goniometric method was carried out with Ni-filtered Cu-Kα radiation at 40 kV × 20 mA and a 2θ scan speed of 16′/min.

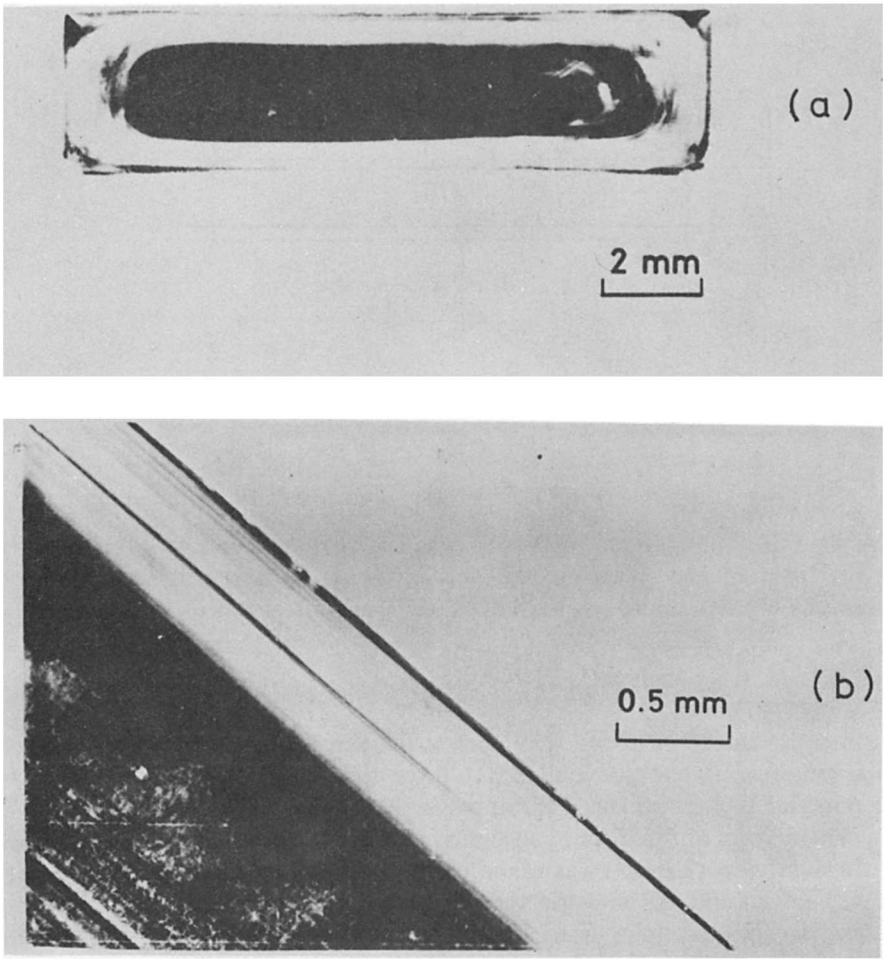

Fig. 2. (a) Polarized micrograph of an injection-molded polypropylene cut perpendicular to flow direction under crossed polars. (b) Enlarged photograph of (a).

Melting Behavior

Melting behavior was measured on the same specimen piece as used for x-ray diffraction using a Perkin Elmer DSC-BI at a scan speed of 10°C/min.

Density

Density was measured on the same specimen piece as used for x-ray diffraction using a water-methanol density-gradient column at 23°C.

Dynamic Viscoelasticity

Skin layer and core layer specimens of about 0.3 mm thickness were sliced from, respectively, the surface and the center of the central parts of the flexural specimens parallel to their surfaces in MD and TD. Dynamic viscoelasticities were measured using a Vibron DDV-II manufactured by Toyo

Baldwin Co., Ltd. at a frequency of 110 cps and a temperature raising rate of 1°C/min.

Tensile Test

Skin layer and core layer specimens of about 0.6 mm thickness were sliced from, respectively, the surface and the center of the central parts of the flexural specimens parallel to their surfaces in MD and TD. Tensile tests were carried out using a Shimazu Autograph IS-5000 with a tensile speed of 100%/min at 23°C.

RESULTS

Observation of Crystalline Texture with Polarizing Microscope

Figures 2(a) and (b) show polarized micrographs of a thin section cut perpendicular to MD. Since these photographs were printed by a quick copier, light and darkness are inverted. Figure 2(a) shows that an injection-molded polypropylene has a clear two-phase structure of skin and core. Figure 2(b), which is an enlarged photograph of Figure 2(a), shows that the skin layer is composed of an outer-oriented amorphous layer and an inner-oriented crystalline layer.

Wide-Angle X-ray Diffraction

Wide-angle x-ray diffraction patterns taken from various directions are shown in Figure 3.

As regards to crystalline structure, the core layer is composed of the α-form (monoclonic form). The skin layer is mostly composed of the α-form, but some coexistence with the β-form (hexagonal form) is also observed (see Fig. 4); a

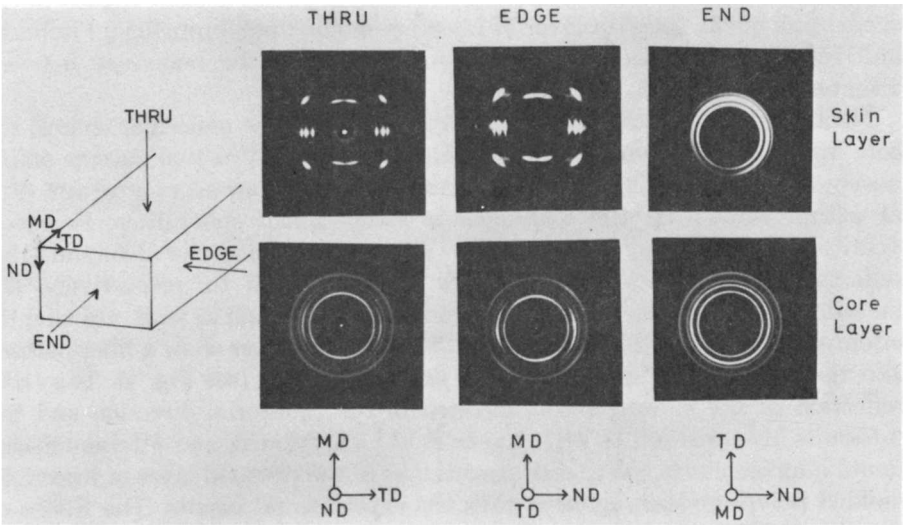

Fig. 3. Wide-angle x-ray diffraction patterns taken from various directions of skin and core layers.

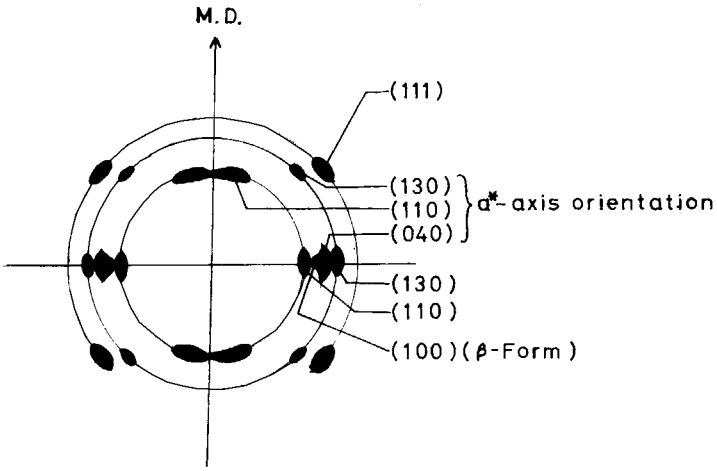

Fig. 4. Schematic interpretation of the wide-angle x-ray diffraction patterns taken from THRU and EDGE views of skin and core layers.

weak reflection is observed inside the (040) reflection of the α-form on the equator, which is the (100) reflection of the β-form. This was confirmed more clearly by a 2θ scan of the skin layer. Awaya[12] reported that the β-form was formed in compression molding after a short melting time at temperature range of 160–180°C which is slightly higher than the melting point. Although the maximum cylinder temperature was 200°C in this experiment, the β-form was formed in the skin layer; it was not formed in the core layer. It is not clear at the present time why the β-form is formed in the skin layer of injection-molded polypropylene. It is necessary to study the specimens injection molded under various conditions. Since the amount of the β-form is small judging from the reflection intensity, it is not essential in analyzing the structure of the skin layer. Kantz et al.[1] found that the β-form existed in the shear zone inside the skin layer of injection-molded polypropylene. Fitchmun and Mencik[13] reported that the β-form existed at the boundary between oriented layer (layer 3) and core layer.

Next, regarding to the orientation state of crystalline molecular chains, the core layer shows Debye rings in its wide-angle x-ray diffraction pattern and is nearly unoriented. This fact is consistent with the polarized micrograph (Fig. 2) which shows that the core layer is composed of spherulites. However, detailed inspection indicates that the (110) reflection and the (040) and (130) reflections of THRU and EDGE are slightly biased to, respectively, the meridional and equatorial directions and the c-axis and a*-axis are slightly oriented to MD. The THRU and EDGE of the skin layer show a fiber pattern and the c-axis and a*-axis are highly oriented to MD (see Fig. 4). The (100) reflection of the β form is concentrated in the equatorial direction and the β-form is also oriented to MD. Kantz et al.[1] and Mencik and Fitchmun[8] also found a mixed c-axis and a*-axis orientation in the oriented layer of injection-molded polypropylene, agreeing with the experimental results. The ENDs of the skin and core layers show Debye rings and molecular chains in them are

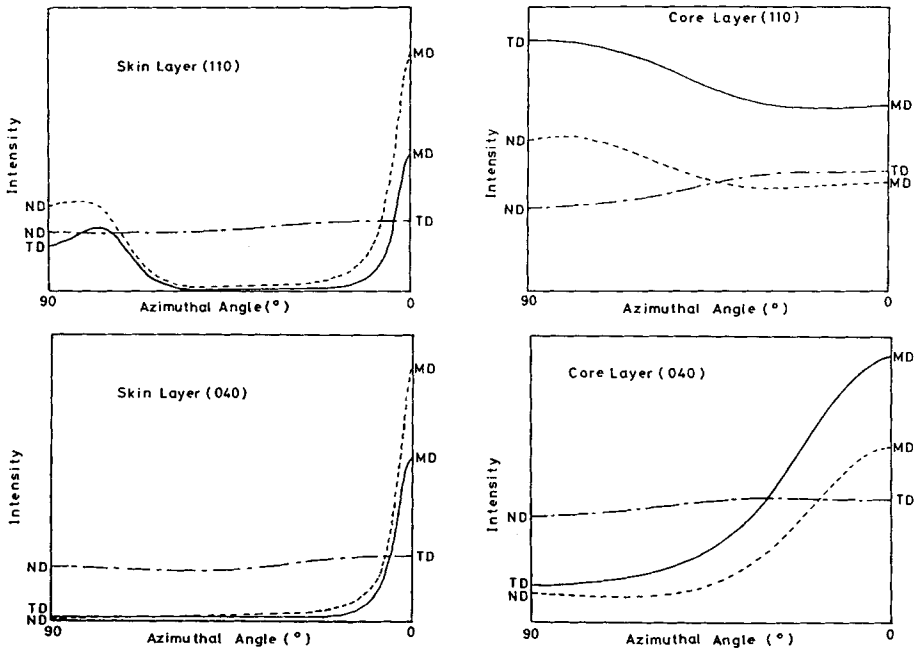

Fig. 5. Azimuthal scans of (110) and (040) reflections measured from various directions of skin and core layers. (—) THRU (MD-TD); (---) EDGE (MD-ND); (—·—) END (TD-ND).

almost unoriented when viewed from MD. Kantz et al.[1] also reported similar results.

The azimuthal scans of the skin and core layers are shown in Figure 5. From the azimuthal scan of the (110) reflection, it can be seen that the c-axis and a*-axis are highly oriented to MD in the THRU and EDGE of the skin layer and the peak of the c-axis-oriented component is sharper than that of the a*-axis-oriented one, indicating that the degree of orientation of the c-axis-oriented component is higher than that of the a*-axis-oriented one. The END shows almost no orientation. The THRU and EDGE of the core layer are in a slightly a*-axis-oriented state and the END shows almost no orientation. Since the skin and core layers are in unoriented states when viewed from MD, their orientation functions can be calculated according to Wilchinsky's method.[10] The orientation functions calculated from Figure 5 are shown in Table I. Since the c-axis-oriented and a*-axis-oriented components are clearly divided in the THRU and EDGE of the skin layer, the fraction of the c-axis-oriented component, [C], and that of the a*-axis-oriented one, [A*], were evaluated in the following manner: a base line was drawn horizontally at the bottom of the azimuthal scan curve of the (110) reflection in Figure 5; the fraction of the area around an azimuthal angle of 0° and that around an azimuthal angle of 90°, out of the area which the azimuthal scan curve and the base line enveloped, were regarded as [C] and [A*], respectively. [C] = 0.382 and [A*] = 0.618 for THRU and [C] = 0.473 and [A*] = 0.527 for EDGE, which indicates that the a*-axis-oriented component is slightly more than the c-axis-oriented one.

TABLE I
Orientation Functions at Various Directions of Skin and Core Layers

Layer	Direction	Orientation function		
		f_a^*	f_b	f_c
Skin	THRU (MD-TD)	−0.114	−0.397	0.512
	EDGE (MD-ND)	−0.178	−0.407	0.585
	END (TD-ND)	−0.025	−0.043	0.068
Core	THRU (MD-TD)	0.076	−0.231	0.155
	EDGE (MD-ND)	0.082	−0.251	0.168
	END (TD-ND)	−0.046	−0.014	0.060

Next, let us examine the orientation functions. As for the skin layer, the orientation functions of END show low values, indicating that the skin layer is in an unoriented state when viewed from MD. THRU and EDGE show positive values of f_c and negative values of f_b and f_a^* and the absolute value of f_a^* is lower than that of f_b. Since the c-axis and a*-axis are highly oriented to MD in the THRU and EDGE of the skin layer as shown in Figures 3 and 5, it is expected that both f_c and f_a^* show positive values. However, f_a^* shows a negative value. The reason for this is as follows: when c-axis-oriented and a*-axis-oriented components coexist, the a*-axis of the c-axis-oriented component and the c-axis of the a*-axis-oriented component are perpendicular to MD. Therefore, when calculating orientation functions, the c-axis of the c-axis-oriented component and the c-axis of the a*-axis-oriented one contradict each other and the a*-axis of the a*-axis-oriented component and the a*-axis of the c-axis-oriented one contradict each other. The signs of the values of f_c and f_a^* are determined by a balance of the amount and orientation degree of the a*-axis-oriented and c-axis-oriented components. In this experiments, although the a*-axis-oriented component is more than the c-axis-oriented one as mentioned above, the degree of orientation of the c-axis-oriented component is higher than that of the a*-axis-oriented one as shown in Figure 5. Therefore, it seems that the orientation degree worked more effectively than the amount and f_c and f_a^* became positive and negative, respectively. The fact that the absolute value of f_a^* is lower than that of f_b is assumed to be due to the contribution of the a*-axis of the a*-axis-oriented component.

As for the core layer, END shows low orientation functions, which means that it is in an unoriented state when viewed from MD. THRU and EDGE show positive values of f_c and f_a^* and negative values of f_b. The absolute values of these orientation functions are lower than those of the skin layer. Although, judging from the azimuthal scan of the (110) reflection in Figure 5, the THRU and EDGE of the core layer seem to have only a*-axis orientation, the calculation of orientation functions shows that f_c is positive, indicating that c-axis-oriented component also exists. This is consistent with the fact that the (130) reflection is slightly biased to the equatorial direction in the wide-angle x-ray diffraction patterns of the THRU and EDGE of the core layer in Figure 3. The facts that END is in an unoriented state and THRU and EDGE show positive values of f_c and f_a^* and negative values of f_b mean

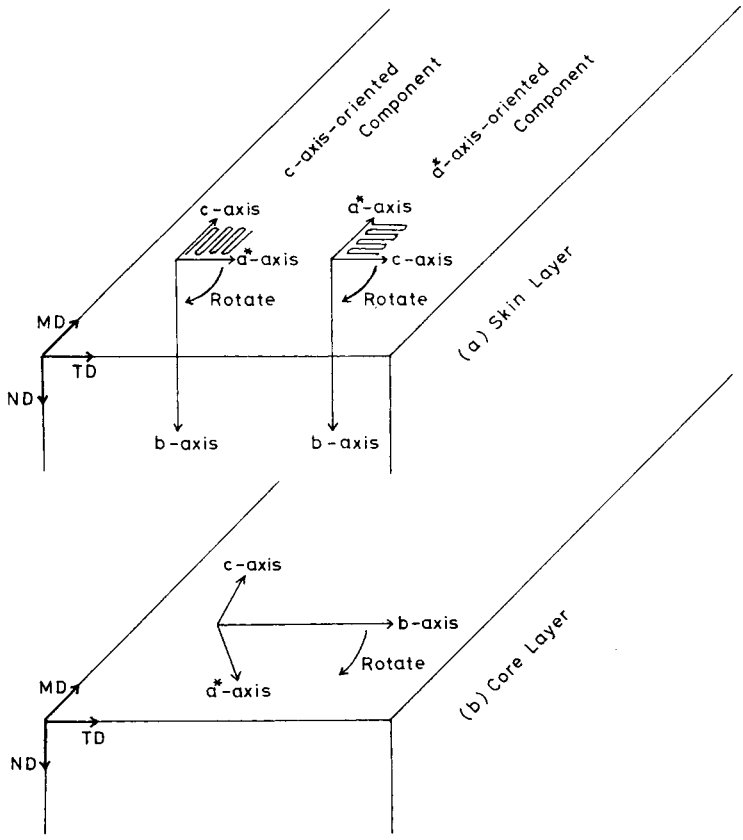

Fig. 6. Orientation states of crystals in (a) skin layer and (b) core layer.

that the b-axis is perpendicular to MD and both the c-axis and a*-axis are not parallel to MD but rotate around MD with an angle to MD. However, since the value of f_b is not so high, the orientation of the core layer seems to be weak in comparison to that of the skin layer.

Figure 6 shows the crystalline orientation states in the skin and core layers assumed from the above-mentioned results.

The crystallinities of the skin and core layers measured with the method described in the experimental section were 50.8% and 55.7%, respectively; the latter was slightly higher. This seems to be due to the slower cooling of the core layer.

Small-Angle X-Ray Scattering

The small-angle x-ray scattering patterns of the skin and core layers taken from THRU are shown in Figure 7. The skin layer shows a clear two-spot pattern in the meridional direction, which indicates the existence of a layer structure. The thickness of the layer calculated from the scattering angle distributes in a range of 100–300 Å; the mean is about 150 Å. The layer structure of about 150 Å thickness easily makes one imagine crystalline lamellae. The two-spot pattern in the meridional direction (MD) indicates

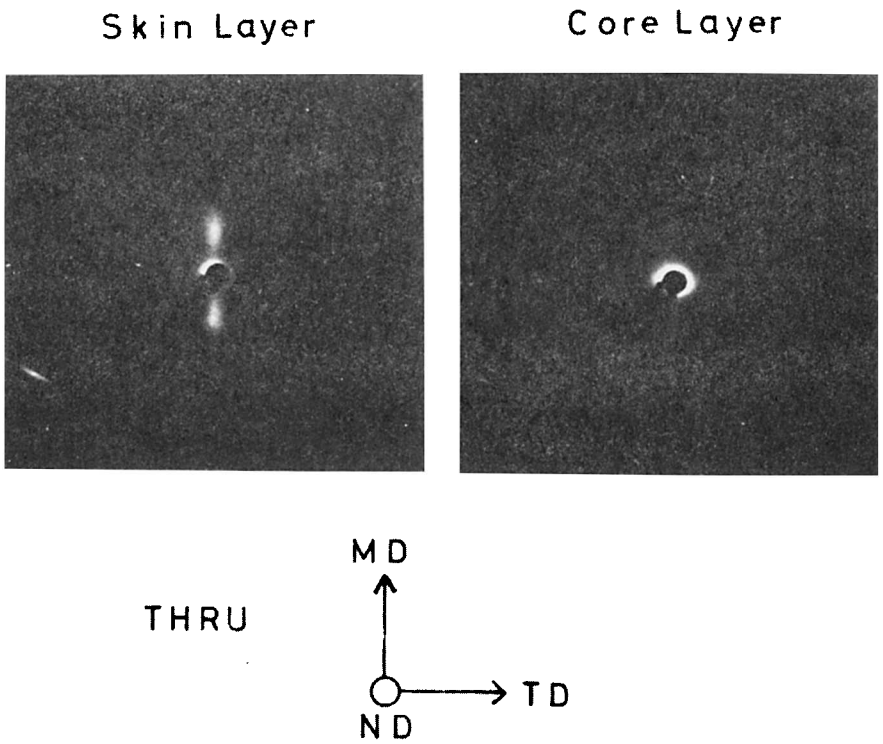

Fig. 7. Small-angle x-ray scattering patterns taken from THRU view of skin and core layers.

that the lamellae are perpendicular to MD. This does not contradict the experimental result that molecular chains are oriented to MD in wide-angle x-ray diffraction. Here, let us consider the a*-axis-oriented lamellae which was observed in wide-angle x-ray diffraction. If a*-axis-oriented lamellae exist, they must be parallel to MD and their c-axes (or plate planes) are considered to rotate at random around MD. Consequently, there must exist a component which is parallel to the incident x-ray beam (or perpendicular to equator), and hence a scattering must be observed on the equator. However, no scattering is observed on the equator in the small-angle x-ray scattering pattern of the skin layer in Figure 7. As a possibility of no scattering on the equator, a case is considered where the plate planes of the a*-axis-oriented lamellae are perpendicular to the incident x-ray beam (or parallel to the surface of molded specimen). However, this case is not probable from the consideration of the growth mechanism of polypropylene crystal[14] where the fold plane is the (010) plane and the growth axis is the a*-axis direction. Since crystallization proceeds from surface to center in injection molding, considering the above-mentioned growth direction of lamella, it seems to be usual that the b-axes point to the surface of molded specimen and the c-axes are parallel to the surface of the molded specimen. However, in actuality, an injection-molded polypropylene is unoriented in END as shown in Figures 3 and 5. Nevertheless, there must exist a component, out of the a*-axis-oriented lamellae, whose plate planes are parallel to the incident x-ray beam. From the fact that no scattering is observed on the equator regardless of the existence of such

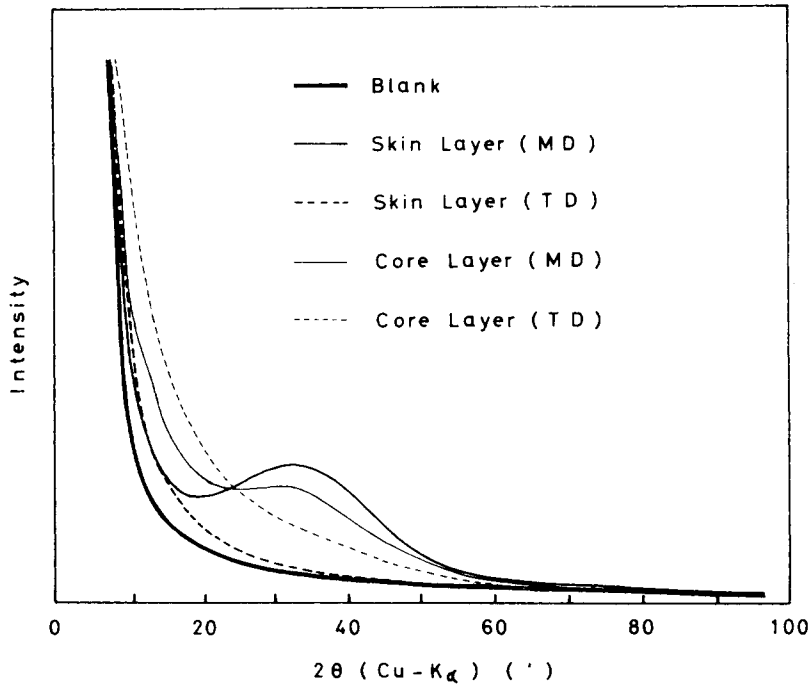

Fig. 8. 2θ scans of small-angle x-ray scattering taken from THRU view along MD and TD of skin and core layers.

component, it is considered that the a*-axis-oriented lamellae are very small in quantity or either small in size or less perfect (or both). Since the a*-axis-oriented component is rather more than the c-axis-oriented component as mentioned before, it seems to be adequate to adopt the latter reason: the lesser perfection of the a*-axis-oriented lamellae. Since the core layer is composed of spherulites and the lamellae in it distribute at random, scattering is observed in all azimuthal angles and hence on the equator too. From the viewpoint of the randomness of lamellae to the equatorial direction, the lamellae in the core layer have higher randomness than the a*-axis-oriented lamellae in the skin layer. The facts that, regardless of the above-mentioned circumstances, a scattering is observed on the equator in the core layer and no scattering is observed on the equator in the skin layer indicate the lesser perfection of the a*-axis-oriented lamellae in the skin layer.

Figure 8 shows 2θ scans of the skin and core layers in THRU. The thickest solid line is for the case of no specimen (blank). When scanning the skin layer in MD (meridional direction of Fig. 7), a strong scattering is observed in a 2θ range of 15–60′ and a peak at $2\theta \doteqdot 33'$. The thickness of the lamellae calculated from this value is about 156 Å. When scanning the skin layer in TD (equatorial direction in Fig. 7), almost no scattering is observed and the scan curve almost agrees with that of the blank. From this, it can be said that the lamellae aligned parallel to MD (a*-axis-oriented lamellae) are not so perfect and uniform as to show a small-angle x-ray scattering.

When scanning the core layer in MD, a shoulder is observed at $2\theta \doteqdot 33'$; a considerable scattering is observed. The thickness of the lamellae calculated

from the scattering angle is also 156 Å: the same as that of the skin layer. When scanning the core layer in TD, although no peak or shoulder is observed, a considerable scattering is observed in a 2θ range of 10–60′ in comparison to the blank, which is in contrast with the TD scan of the skin layer.

Melting Behavior

The DSC thermograms of the skin and core layers of an injection-molded polypropylene and a compression-molded polypropylene are shown in Figure 9. All thermograms are normalized on a same sample weight. An endotherm begins at about 120°C and peaks are observed at 162–165°C. The peak temperatures are: compression-molded, 162.5°C; core layer, 164.5°C; skin layer, 165.5°C; the difference between the peak temperature of the skin layer and that of the core layer is only 1°C. However, the temperatures at which endotherms end are: compression-molded, 170°C; core layer, 170°C; skin layer, 182°C; the skin layer has a high temperature melting component. The fraction of this component which melts above 170°C was calculated from the area of the thermogram to be about 5.3%.

Density

The densities at 23°C of an injection-molded polypropylene are: core layer, 0.9067 g/cm^3; skin layer, 0.9073 g/cm^3; the skin layer has a slightly higher density than the core layer. As mentioned before, the crystallinity of the skin layer measured with x-ray diffraction is lower than that of the core layer. The fact that the skin layer has a slightly higher density than the core layer regardless of its low crystallinity means that the amorphous chains are strained in the skin layer.

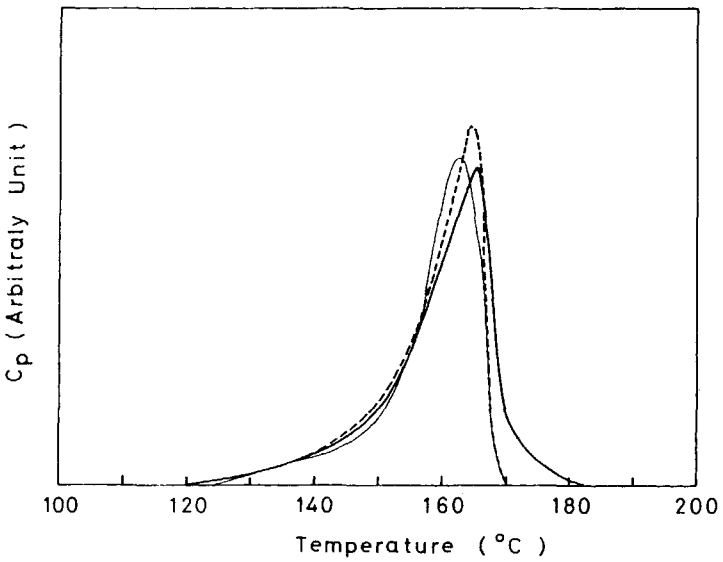

Fig. 9. DSC thermograms of skin (—) and core layers (---) of injection-molded polypropylene and compression-molded (—) polypropylene.

Dynamic Viscoelasticity

Figure 10(a) shows the temperature dependences of dynamic modulus E' and loss modulus E''. Although the skin and core layers show similar E' at low temperature, the skin layer shows higher E' than the core layer at high temperature. The dynamic modulus of the skin layer, E_s', at room temperature (23°C) is 2.0×10^{10} dyn/cm^2, that of the core layer, E_c', is 1.5×10^{10} dyn/cm^2, and $E_s'/E_c' \doteqdot 1.3$. At 100°C, $E_s'/E_c' \doteqdot 2.0$; the skin layer shows a value of E' about twice that of the core layer. Although the skin layer already shows a higher modulus than the core layer at room temperature, the decrease

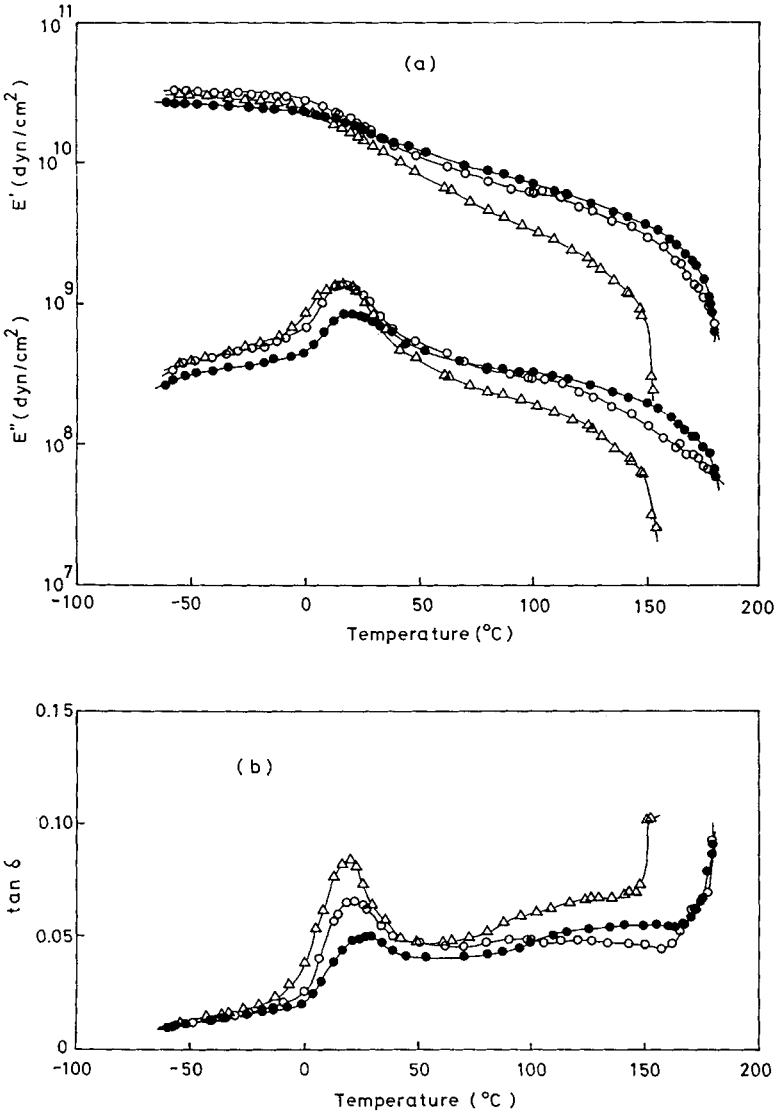

Fig. 10. Temperature dependences of (a) dynamic modulus E' and loss modulus E'' and (b) loss tangent tan δ of skin and core layers of an injection-molded polypropylene. (○) Skin layer (MD); (●) skin layer (TD); (△) core layer (MD).

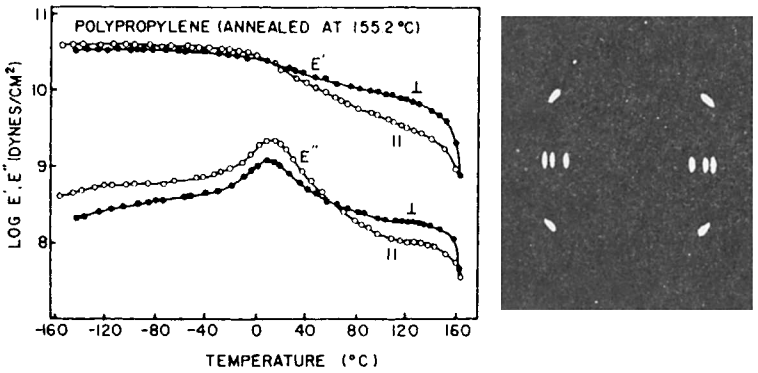

Fig. 11. Temperature dependences of E' and E'' along and perpendicular to drawing direction for a cold-drawn and annealed polypropylene. X-ray diffraction pattern is for the same sample.[15]

of the modulus of the skin layer with rising temperature is lower than that of the core layer, suggesting that the molding with thick skin layer gives high modulus and high thermal resistance. As shown in the previous papers,[2-4] this can be done, for example, by molding a high molecular weight resin at a low cylinder temperature. Next, while the sudden drop of E' caused by melting occurs at about 150°C for the core layer, it occurs at about 180°C for the skin layer: about 30°C higher for the skin layer. Although, for the skin layer, the final temperature at which E' suddenly drops corresponds well to the melting point measured thermally with differential scanning calorimetry (DSC), the drop of E' already occurs at a considerably early stage of thermal melting for the core layer.

Next, let us consider the anisotropy of E' of the skin layer. Comparison between E' in MD and that in TD of the skin layer shows that, although the former is higher in the temperature range below 33°C which is a temperature slightly higher than the primary absorption temperature (about 20°C), the order reverses above 33°C. The final sudden drop of E' occurs at the same temperature of about 180°C in both MD and TD. The fact that E' in MD and that in TD cross at a temperature slightly higher than the primary absorption temperature has been reported for cold-drawn and annealed semicrystalline polymers by Takayanagi et al.[15] Figure 11 shows a reproduction of Takayanagi et al.'s results for a polypropylene cold-drawn and annealed at 155.2°C. Takayanagi et al. have shown that the fact that E' in MD and that in TD cross at a temperature slightly higher than the primary absorption temperature can be interpreted when the series connection of C and A is strong in a mechanical model with crystalline region (C) and amorphous region (A) as shown in Figure 12(a), and proposed a modified model of Hosemann[16] as shown in Figure 12(b) as a structural model for cold-drawn and annealed semicrystalline polymers. The crossing of E' in MD and that in TD of the skin layer observed in this experiment also can be interpreted by such a model.

Figure 10(b) shows the temperature dependence of loss tangent $\tan\delta$. Comparing $\tan\delta$ in MD of the skin layer and that of the core layer, the primary absorption peak temperature of the skin layer is about 2°C higher than that of the core layer and the primary absorption peak of the skin layer

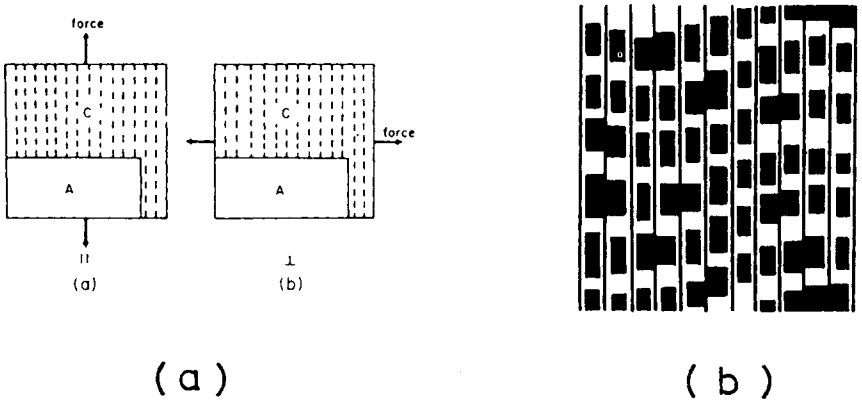

Fig. 12. (a) Mechanical model of crystalline polymer, which illustrates the different ways of response when the force is applied (a) along and (b) perpendicular to the molecular axis. The direction of molecular chains is represented by broken lines. (b) Structural model which interprets the actual dispersion behavior of cold-drawn and annealed crystalline polymers. Amorphous regions are expressed by black areas.[15]

is smaller than that of the core layer. This means that the amorphous molecular chains in the skin layer are more extended and strained than that in the core layer, and is consistent with the fact that the density of the skin layer is higher than that of the core layer regardless of its lower x-ray crystallinity as mentioned before. The crystalline absorption of the skin layer is weaker than that of the core layer, which originates in the lower crystallinity of the skin layer. While the core layer shows a final rise of tan δ by melting at about 150°C, the skin layer shows an omen phenomenon of melting from about 160°C and a final rise of tan δ at about 180°C.

As for the anisotropy of tan δ of the skin layer, the primary absorption peak temperature in TD is about 7°C higher than that in MD and the primary absorption peak in TD is smaller than that in MD. This is assumed to be due to the fact that, since in MD the series connection of C and A is stronger than the parallel connection of C and A in Takayanagi et al.'s mechanical model, the character of A region appears stronger in MD than in TD. As for crystalline absorption, both the absorption temperature and intensity are higher in TD than in MD. This is assumed to be because the parallel connection of C and A in TD is stronger than the series connection of C and A in Takayanagi et al.'s mechanical model, the character of C region appears stronger in TD than in MD. The final rise of tan δ by melting occurs at about 180°C in both MD and TD.

Tensile Property

Figure 13 shows the stress–strain curves of the skin and core layers. The skin layer in MD shows a very high yield stress with a dull yielding peak, ruptures just after yielding, and does not show necking. The core layer in MD shows a low yield stress with a sharp yielding peak and shows a long necking before rupture. The stress-strain curve of the core layer is similar to that of compression-molded specimen. The skin layer in TD shows a further lower yield stress than the core layer in MD and shows necking before rupture. The

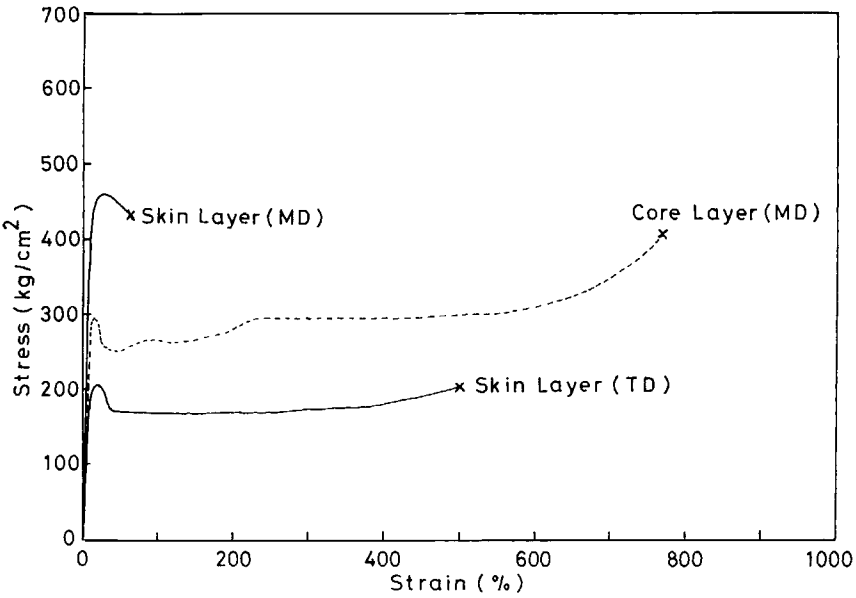

Fig. 13. Stress-strain curves of the skin (—) and core (---) layers of an injection-molded polypropylene.

necking stress of the skin layer in TD is lower than that of the core layer in MD. The yielding peak of the core layer in MD is sharper than that of the skin layer in TD. The yield stress of the skin layer in TD is less than half that in MD.

DISCUSSION

From the above experimental results, it has become apparent that, in the skin layer, lamellae are perpendicular and parallel to flow direction (MD) and there are crystallites with a high melting temperature and high strength. In general, a polypropylene melt crystallizes under a high shear stress in injection molding. This is particularly notable near the surface. Therefore, it is considered appropriate to apply a shishkebab structure [Fig. 14(b)] proposed by Keller and Machin[17] to the structure of the skin layer. Figure 15 shows a modified shishkebab structure drawn to fit the actual case on consideration of the above results. Crystalline lamellae, which are "kebabs" fill space, and fibrous crystals which are "shishes" penetrate them in MD. Some kebabs are linked up with neighboring kebabs. Although only shishes are drawn in Figure 15 as linkage in MD, it is considered that, in actuality, there also exist tie molecules which link the kebabs in MD. Small and nonuniform lamellae whose a*-axes are parallel to MD pile epitaxially on the c-axis-oriented lamellae which are a component (kebabs) of the shishkebab main skeleton structure. The a*-axis-oriented imperfect lamellae are rather larger in quantity than the c-axis-oriented perfect lamellae. Although some β-form crystallites also exist, these may be regarded as an accessory. Amorphous chains fill the space of the above-mentioned crystalline structure. The amount of the amorphous chains is about a half of the total volume.

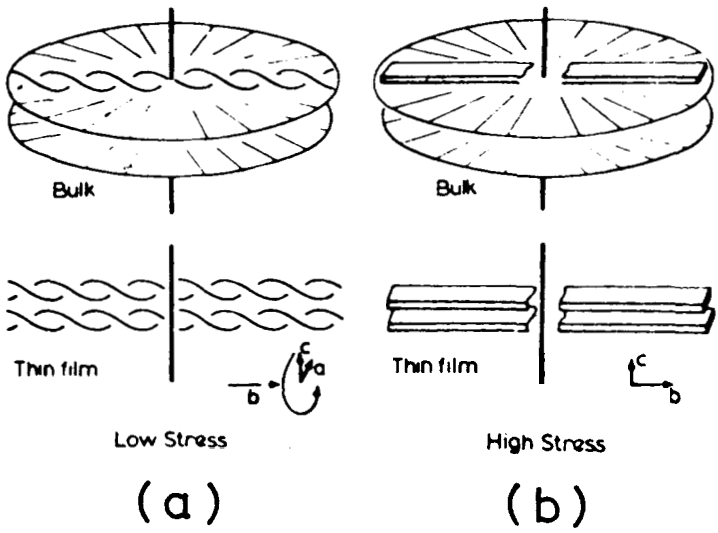

Fig. 14. Models of polyethylene crystals crystallized from melts under (a) low shear stress and (b) high shear stress.[17]

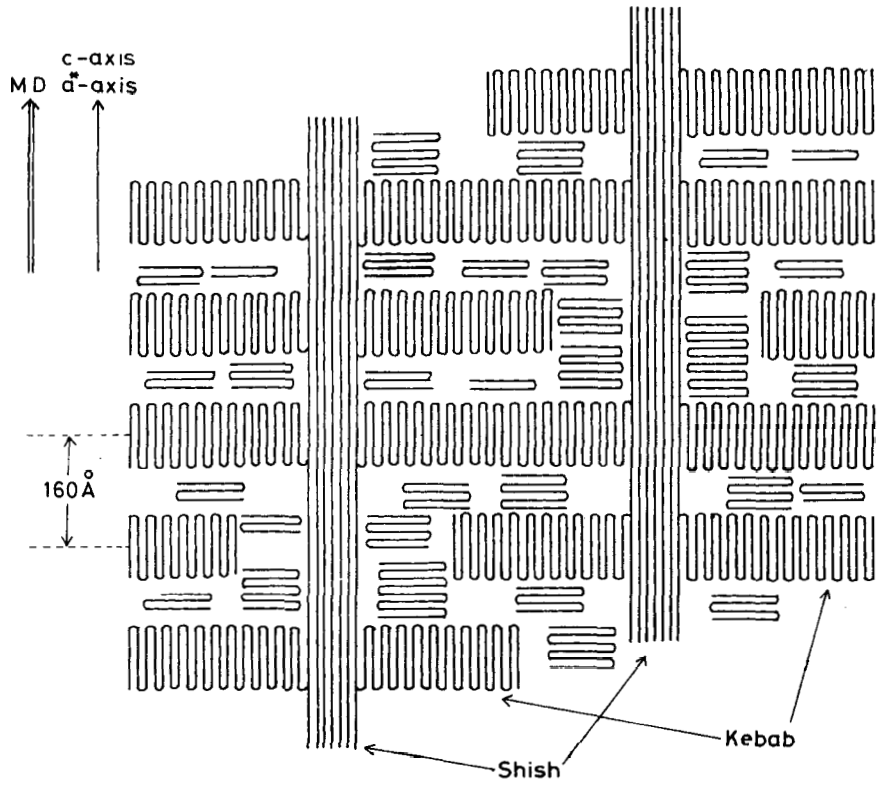

Fig. 15. Proposed structural model of skin layer in injection-molded polypropylene.

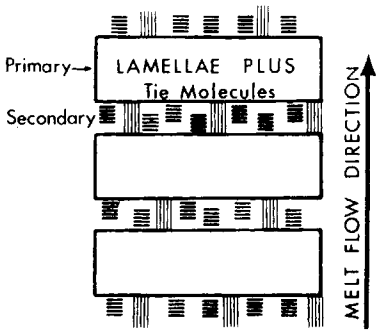

Fig. 16. Morphology of skin layer in injection-molded polypropylene with bimodal orientation (schematic), showing primary and secondary crystallization stages.[18]

In order to interpret the molded-in hinge of injection-molded polypropylene, Clark and Spruiell[18] proposed a model shown in Figure 16 as a structure of skin layer in injection-molded polypropylene, based on the previous studies on the mixed c-axis and a*-axis orientation seen in such as melt-spun polypropylene fiber and their own x-ray study on the skin layer in injection-molded polypropylene. In this model, the primary component consists of a row structure of planar lamellae interconnected by a fraction of tie molecules, whose c-axis is oriented to flow direction, and the secondary component consists of interlamellar crystals of small size and lower crystallinity oriented by epitaxy with respect to the planar lamella substrate of the primary component, which have been formed by the secondary crystallization of the rejected molecular chains at primary crystallization and whose a*-axes are oriented to flow direction. They have interpreted the molded-in hinge as being the secondary component which acts as a morphological plasticizer. Our model, shown in Figure 15, which has been assumed from various experimental results such as structural analyses and measurements of thermal and mechanical properties, etc. is, as a result, very similar to Clark and Spruiell's model shown in Figure 16 which has been assumed from purely structural speculation. The main difference between them is that, while Clark and Spruiell assign tie molecules to the linkage of lamellae in flow direction, we assign shishes in addition to tie molecules.

The structure shown in Figure 15 must show a mixed c-axis and a*-axis orientation in its wide-angle x-ray diffraction pattern. Since the c-axis-oriented lamellae are perpendicular to MD, its small-angle x-ray scattering must show a two-spot pattern on the meridian. Since the a*-axis-oriented lamellae are small, nonuniform, and imperfect, almost no scattering is observed on the equator.

In general, the melting point of a semicrystalline polymer is higher as the thickness of lamellae, l, is larger. Since the shishes in Figure 15 are fibrous crystals with large l, the structure shows a high melting component in its melting behavior. In general, l is larger as crystallization temperature is higher. Since, in injection molding, the skin layer is rapidly cooled and the core layer is cooled more slowly, the crystallization temperature in the skin layer is lower than that in the core layer. Thus, l must be smaller in the former than in the latter and the melting point must be rather lower in the

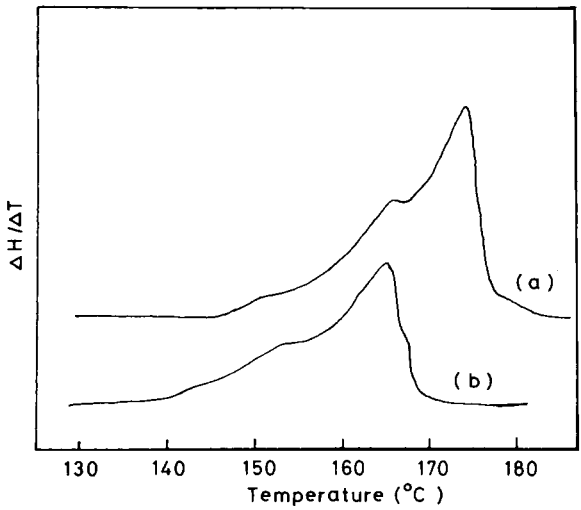

Fig. 17. DSC thermograms of polypropylenes crystallized from solution. (a) Fibrous crystals, α-chloronaphthalene, 1%, 126°C, revolution speed of stirring; 300 rpm. (b) Single crystals, α-chloronaphthalene, 0.3%, 120°C, no stirring.[19]

former. However, the experimental results show a reverse tendency: the skin layer shows a higher melting point than the core layer; in particular, there exists a component whose melting point is 12°C higher than that of the core layer. Such a high melting point crystal is not formed from usual crystallization under ambient conditions. However, crystallization occurs under a high pressure and high shear stress in injection molding; good conditions for the formation of shishkebab structure are all present. From the above-mentioned facts, it may be appropriate to assign the high melting point crystals to shishes. Monobe et al.[19] have shown that, in the melting behavior in DSC of solution-crystallized polypropylenes, fibrous crystals formed by stirred crystallization show a melting peak at 173°C and complete melting at about 182°C while single crystals show a melting peak at 164°C and complete melting at 170°C (see Fig. 17). These are valid data supporting the existence of shishes in this experiment.

Next, the fact that the dynamic modulus, E', of the skin layer holds high value even above the temperature (160°C) where most crystals melt in thermal measurement seems to be due also to the existence of shishes. The reason is that the shishes which are fibrous crystals, have a high modulus, and long penetrate the texture in MD, must hold most of stress. Accordingly, even after melting of low melting point lamellae, the shishes and residual lamellae of high melting point hold the stress and maintain high modulus. The model shown in Figure 15, from a mechanical viewpoint, has a strong series connection of C and A in Figure 12 shown by Takayanagi et al.[15] and can interpret a crossing of E' in MD and that in TD at a temperature slightly higher than the primary absorption temperature.

A high yield stress of the skin layer in MD is also considered to be due to the shishes which, because of fibrous crystals, have a high strength and deeply penetrate the texture. The fact that the skin layer in MD ruptures just after

yielding and does not show necking in tensile test is assumed to be because the kebabs which are a main component of the crystalline structure of the skin layer are perpendicular to MD as shown in Figure 15, a rotation of lamellae to tensile direction (MD) is difficult and thus unfolding of molecular chains is also difficult. The existence of the shishes makes it still more difficult. The yield stress of the skin layer in TD is less than half that in MD and is lower than that of the core layer in MD. The reason for this is that since the c-axis of the shishkebab structure which is the main skeleton of the skin layer is parallel to MD, its resisting force to stress in TD is van der Waals force and thus the skin layer in TD is deformed with a weak force when it is pulled. Although the a*-axis-oriented lamellae point their c-axes to TD, they are imperfect and not connected in TD, and thus have only a low resisting force to stress and contribute little to yield stress. The necking stress of the skin layer in TD is lower than that of the core layer in MD. Since the c-axis of the shishkebab structure is parallel to MD, unfolding of molecular chains is easy in TD. Since the core layer is composed of spherulites and the lamellae in it distribute at random, its resisting force to deformation should be larger than that of the skin layer in TD, and thus the yield and necking stresses of the skin layer in TD are lower than those of the core layer.

Lastly, let us discuss a formation mechanism of the model shown in Figure 15. Since a molten resin near the cavity surface is applied a high shear stress in injection molding, the molecular chains in it are extended. On crystallization by cooling, molecular chains with a high degree of extension gather first and form fibrous crystals and, then, molecular chains with a lower degree of extension pile on the fibrous nuclei by chain folding. Thus, a shishkebab structure is formed. At this time, a part of molecular chains are rejected from forming lamellae, remain in the space of the main skeleton structure, then do a secondary crystallization and pile epitaxially on the main skeleton structure. Thus, a*-axis-oriented imperfect lamellae are formed. Katayama et al.[20] have shown that a highly c-axis-oriented component is formed first and an a*-axis-oriented component is formed at a later time in melt-spinning of polypropylenes.

CONCLUSIONS

An injection-molded polypropylene shows a clear skin/core structure when observed with a polarizing microscope. The structures of the skin and core layers have been clarified from the measurements of melting behavior, density, dynamic viscoelasticity and tensile property in addition to polarizing microscopy, wide-angle x-ray diffraction and small-angle x-ray scattering. It has been concluded that the core layer is composed of spherulites, the crystals in which have weak c-axis and a*-axis orientations in MD and the skin layer is composed of shishkebab-like main skeleton structure, whose axis is parallel to MD, piled epitaxially with a*-axis-oriented imperfect lamellar substructure.

References

1. M. R. Kantz, H. D. Newman, Jr., and F. H. Stigale, *J. Appl. Polym. Sci.*, **16**, 1249 (1972).
2. M. Fujiyama and S. Kimura, Kobunshi Ronbunshu, **32**, 581 (1975).
3. M. Fujiyama and S. Kimura, Kobunshi Ronbunshu, **32**, 591 (1975).

4. M. Fujiyama, H. Awaya, and S. Kimura, *J. Appl. Polym. Sci.*, **21**, 3291 (1977).
5. M. Fujiyama and S. Kimura, *J. Appl. Polym. Sci.*, **22**, 1225 (1978).
6. E. S. Clark, *SPE J.*, **23**(7), 46 (July, 1967).
7. E. S. Clark, Paper presented at meeting of the American Physical Society, Dallas, 1970.
8. Z. Mencik and D. R. Fitchmun, *J. Polym. Sci.; Polym. Phys. Ed.*, **11**, 973 (1973).
9. K. Matsumoto, I. Miura and K. Hayashida, Kobunshi Ronbunshu, **36**, 401 (1979).
10. Z. W. Wilchinsky, *J. Appl. Phys.*, **31**, 1969 (1960).
11. A. Weindinger and P. H. Hearmans, *Makromol. Chem.*, **50**, 98 (1961).
12. H. Awaya, Nihon Kagaku Zasshi, **83**, 865 (1962).
13. D. R. Fitchmun and Z. Mencik, *J. Polym. Sci.; Polym. Phys. Ed.*, **11**, 951 (1973).
14. M. Kojima, *J. Polym. Sci., A-2*, **5**, 597 (1967).
15. M. Takayanagi, K. Imada, and T. Kajiyama, *J. Polym. Sci.; Part C*, (15), 263 (1966).
16. R. Hosemann, *J. Appl. Phys.*, **34**, 25 (1963).
17. A. Keller and M. J. Machin, *J. Macromol. Sci.,-Phys.*, **B2**, 501 (1968).
18. E. S. Clark and J. E. Spruiell, *Polym. Eng. Sci.*, **16**, 176 (1976).
19. K. Monobe, Y. Fujiwara, and Y. Yamashita, *Kogyo Kagaku Zasshi*, **73**, 1420 (1970).
20. K. Katayama, T. Amano, and K. Nakamura, *Kolloid Z.-Z. Polymere*, **226**, 125 (1968).

Received March 10, 1987
Accepted April 28, 1987